Aldehyde Surface-Functionalized Shell Cross-Linked Micelles with pH-Tunable Core Swellability and Their Bioconjugation with Lysozyme

Hao Liu, Xiaoze Jiang, Jun Fan, Guanghui Wang, and Shiyong Liu*

Department of Polymer Science and Engineering, Joint Laboratory of Polymer Thin Films and Solution, School of Life Science, Hefei National Laboratory for Physical Sciences at the Microscale, University of Science and Technology of China, Hefei, Anhui 230026, China

Received July 6, 2007; Revised Manuscript Received August 27, 2007

ABSTRACT: Two approaches were attempted for the syntheses of α-aldehyde terminally functionalized double hydrophilic diblock or triblock copolymers of 2-(dimethylamino)ethyl methacrylate (DMA), 2-(diethylamino)-ethyl methacrylate (DEA), and oligo(ethylene glycol)methyl ether methacrylate (OEGMA) via an atom transfer radical polymerization (ATRP) process. The first approach employed 2-(2,2-dimethoxyethoxy)ethyl α-bromoisobutyrate as the ATRP initiator for the sequential polymerization of DMA and DEA monomers. However, after deprotection of the terminal acetal into aldehyde groups, the obtained *Ald*-PDMA-*b*-PDEA diblock copolymer was prone to aldol condensation at alkaline pH, leading to extensive formation of dimers. Directly using 4-aldehydephenyl α-bromoisobutyrate as the ATRP initiator, the sequential polymerization of OEGMA, DMA, and DEA led to the successful preparation of the α-aldehyde terminally functionalized triblock copolymer, *Ald*-POEGMA-*b*-PDMA-*b*-PDEA. This triblock copolymer molecularly dissolves in acidic media and self-assembles into three-layer onion-like micelles consisting of PDEA cores, PDMA inner shells, and POEGMA outer coronas at alkaline pH. Selective cross-linking of the PDMA inner shell with 2-bis(2-iodoethoxy)ethane led to structurally stabilized shell cross-linked (SCL) micelles functionalized with surface aldehyde groups. Possessing the PDEA cores, the obtained SCL micelles exhibited reversible pH-responsive swelling/deswelling behavior, as revealed by dynamic laser light scattering. The surface aldehyde groups of SCL micelles enabled their facile conjugation with a model protein, lysozyme, via the formation of Schiff bases. The micelle−protein bioconjugate was characterized by sodium dodecyl sulfate-polyacrylamide gel electrophoresis. The previous results suggest promising applications of SCL micelles in fields such as targeted drug delivery and controlled release.

Introduction

During the past decade, ever-increasing attention has been paid to the development of novel drug delivery systems to achieve enhanced bioavailability of drugs with negligible side effects, especially in the field of cancer chemotherapy.[1−8] However, successful results have not always been obtained due to problems associated with drug carriers, such as recognition by the reticuloendothelial system and nonspecific deposition in the body before their arrival at the target sites. The crucial point to solving these problems is the fabrication and development of suitable drug carriers to attain stable circulation in the blood compartments, preferential accumulation at the designated area, and the subsequent smart/controllable release.[2,7]

Amphiphilic block copolymers can self-assemble in aqueous solution into aggregates with various morphologies, such as micelles[9,10] or vesicles.[11] As the hydrophobic core can enhance the solubility of small molecule drugs, block copolymer micelles can thus act as suitable drug nanocarriers.[1,2,7,8] To achieve targeted drug delivery, the surface of the self-assembled micelles needs to be functionalized with bioactive pilot molecules such as peptide,[12−16] folate,[17−20] and saccharide,[21−24] which can modulate the biodistribution of nanocarriers and induce specific cellular uptake by receptor-mediated endocytosis. Thus, reactive groups such as aldehydes[16,22,25−31] and carboxyls[13,14,19,21,24,32−35] need to be first introduced at the chain end of the hydrophilic block of amphiphilic block copolymers. Kataoka et al.[15,16,20,22,23,28−31] have extensively investigated the preparation of micelles from PEO-based amphiphilic block copolymers with reactive aldehyde groups at the terminal end of the PEO block. The aldehyde groups at the micelle surface allow their further conjugation with pilot molecules.[15,16,20,22,23,28]

Another important consideration concerning the practical applications of amphiphilic block copolymer micelles in the field of targeted drug delivery is their circulation stability in the blood compartments. Amphiphilic block copolymer micelles will inevitably disintegrate into unimers when the copolymer concentration falls below the critical micelle concentration (cmc), which can typically occur due to large dilution after the administration of drug-containing nanocarriers. This will lead to premature release of the active compounds.

To account for the stability issue of amphiphilic block copolymer micelles, core cross-linking (CCL)[25,32,36−43] or shell cross-linking (SCL)[12−14,19,21,33−35,44−60] approaches have been developed. The latter was originally reported by Wooley et al. in 1996.[44] Moreover, the periphery of SCL micelles can be further functionalized with reactive groups for the conjugation with targeting agents.[12−14,19,21,48−52] Wooley et al.[48] recently reported the preparation of well-defined biotin-terminated poly(acrylic acid)-*b*-poly(methyl acrylate) (*Biotin*-PAA-*b*-PMA), which can self-assemble in aqueous solution into a stable and uniform micelle nanoparticle surface attached with biotin. They further investigated the competitive binding of the obtained SCL micelles with avidin. The residual carboxyl groups of SCL micelles can also be employed to attach fluorescent labels,[12,13,34,49] folate,[19] and/or conjugation with short peptide[12−14] or DNA sequences.[35,52]

* Corresponding author. E-mail: sliu@ustc.edu.cn.

10.1021/ma071494o CCC: $37.00
Published on Web 11/10/2007

In almost all the previous cases, amphiphilic block copolymers were employed for the fabrication of core−shell nanoparticles, and there exist two major limitations. First, a cosolvent approach is typically employed to induce the micellization in aqueous solution, and the complete removal of organic solvent molecules through a tedious and time-consuming dialysis procedure is necessary. Second, the micelle cores were essentially hydrophobic, and only water-insoluble drugs could be solubilized and delivered. Although targeted delivery and preferential accumulation at targeted sites can be achieved, the release profile of the encapsulated drugs cannot be well-controlled.

Recent progresses in the field of double hydrophilic block copolymers (DHBCs) seem to be able to provide a suitable solution to the previous problems. DHBCs can be directly dispersed in aqueous solution at certain conditions; upon changing the external conditions, such as pH,[27,55,56,59,61−74] temperature,[63,69,71,75] and ionic strength,[70,72,73] one of the blocks of DHBCs can be selectively rendered water-insoluble, while the other block still remains well-solvated to stabilize the formed colloidal aggregates. Most importantly, the unimer-to-micelle transition can be fully reversible, providing chances of triggered release of initially solubilized guest molecules within hydrophobic cores. It should be noted that the structural integrity of DHBC micelles can be facilely achieved by SCL, which has been extensively investigated by Armes et al.[53−60]

The unique properties of DHBCs augur for their promising applications in the field of targeted drug delivery and triggered release. Most pathological processes exhibit either a slight increase in temperature or a decrease in pH.[2] For instance, contrary to the normal blood pH of 7.4, extracellular pH values in tumorous tissues are ca. 6.5−7.0.[76] Moreover, drug nanocarriers can enter living cells via endocytosis, and the intracellular environment is typically acidic (pH 5−6).[20] Thus, it is relatively convenient to manipulate the pH stimulus both in vitro and in vivo.[77]

The pH-responsive DHBCs containing ionizable blocks with tunable water solubility, such as poly(acrylic acid) (PAA),[61−63] poly(methacrylic acid) (PMAA),[64] and poly(2-(diethylamino)-ethyl methacrylate) (PDEA),[56,67,68,71] have been extensively studied. Poly(ethylene oxide)-*b*-poly(2-(dimethylamino)ethyl methacrylate)-*b*-poly(2-(diethylamino)ethyl methacrylate) (PEO-*b*-PDMA-*b*-PDEA) triblock copolymers were found to self-assemble into micellar structures at physiological pH.[56,67] The hydrophobic PDEA cores can efficiently solubilize hydrophobic drugs (i.e., dipyridamole).[67] Acidification of the aqueous solution provoked the protonation of tertiary amine residues and resulted in the dissociation of PDEA−core micelles into unimers, accompanied with the rapid in vitro release of encapsulated drugs at pH < 6.5. However, in this intriguing system, two important issues (i.e., micelle stability and surface functionalization with bioactive pilot molecules for targeted delivery) have not been considered.

Herein, we report a novel drug nanocarrier system fabricated from a pH-responsive DHBC. As compared to conventional delivery vehicles of amphiphilic block copolymer micelles, they possess four distinct advantages at the same time: structural stability due to SCL, pH-tunable core swelling/shrinkage for controlled release of encapsulated guest molecules, biocompatibility and nontoxicity due to the POEGMA outer corona, and versatility of surface conjugation due to the presence of reactive groups at the periphery.

We synthesized the α-aldehyde terminally functionalized DHBC of oligo(ethylene glycol)methyl ether methacrylate (OEGMA), 2-(dimethylamino)ethyl methacrylate (DMA), and 2-(diethylamino)ethyl methacrylate (DEA) via a sequential atom transfer radical polymerization (ATRP) technique using a aromatic aldehyde-containing initiator (Scheme 1). The obtained triblock copolymer, *Ald*-POEGMA-*b*-PDMA-*b*-PDEA, molecularly dissolves in acidic media and supramolecularly self-assembles into three-layer onion-like micelles consisting of a pH-sensitive PDEA core, a cross-linkable PDMA inner layer, and a biocompatible POEGMA outer corona at alkaline pH. The SCL reaction was facilely conducted upon addition of difunctional 2-bis(2-iodoethoxy)ethane (BIEE). The pH-responsive micellization, SCL, and pH-tunable core swellability of the obtained SCL micelles were investigated in detail by surface tension, ^{1}H NMR, dynamic laser light scattering (LLS), and transmission electron microscopy (TEM). Moreover, the presence of aldehyde groups at the periphery of SCL micelles allows for the successful conjugation with lysozyme. The micelle−protein bioconjugate was characterized by sodium dodecyl sulfate-polyacrylamide gel electrophoresis (SDS-PAGE). It should be noted that this proof-of-concept demonstration reveals that surface-functionalized SCL micelles of stimuli-responsive DHBCs may find practical applications in the fields of targeted drug delivery and smart release.

Experimental Procedures

Materials. Oligo(ethylene glycol)methyl ether methacrylate (OEGMA, $M_n = 475$, mean degree of polymerization, DP, is 8−9) was passed through an alumina column to remove the inhibitor. 2-(Dimethylamino)ethyl methacrylate (DMA, Acros) and 2-(diethylamino)ethyl methacrylate (DEA, Aldrich) were vacuum-distilled from CaH_2. All monomers were stored at −20 °C prior to use. Tetrahydrofuran (THF) was dried by refluxing over sodium/benzophenone and distilled prior to use. Triethylamine (TEA), methanol (MeOH), and isopropyl alcohol (IPA) were dried over CaH_2 and distilled at reduced pressure. 4-Hydroxybenzaldehyde (98%, Shanghai Chemical Reagent Co.) was recrystallized twice from H_2O. Chloroacetaldehyde dimethyl acetal (97%, Acros), α-bromoisobutyryl bromide (98%, Aldrich), copper(I) bromide (CuBr, 98%, Aldrich), 2,2′-bipyridine (bpy, 99+%, Aldrich), 2-bis-(2-iodoethoxy)ethane (BIEE, 96%, Aldrich), egg white lysozyme (14.6 kDa, Amresco), and other reagents were used as received. 2-(2,2-Dimethoxyethoxy)ethyl α-bromoisobutyrate (*Acetal*-Br) and 4-formylphenyl α-bromoisobutyrate (*Ald*-Br) were prepared from chloroacetaldehyde dimethyl acetal[78] and 4-hydroxybenzaldehyde,[26,27,79] respectively.

Sample Preparation. The general approaches to the preparation of aldehyde terminally functionalized diblock and triblock copolymers are shown in Scheme 1.

Synthesis of α-Aldehyde Terminally Functionalized PDMA-*b*-PDEA Diblock Copolymer (*Ald*-PDMA-*b*-PDEA). α-Aldehyde terminally functionalized PDMA-*b*-PDEA diblock copolymer, *Ald*-PDMA-*b*-PDEA, was synthesized by sequential ATRP polymerization of DMA and DEA monomers using *Acetal*-Br as the initiator, followed by deprotection. In a typical example, *Acetal*-Br (0.138 g, 0.46 mmol), bpy ligand (0.144 g, 0.92 mmol), and DMA monomer (4.34 g, 27.6 mmol) were charged into a reaction flask containing 5 mL of MeOH. The flask was degassed via three freeze−thaw−pump cycles and back-filled with N_2. CuBr (66 mg, 0.46 mmol) was introduced into the reaction flask under the protection of N_2 flow to start the polymerization at ambient temperature under N_2 atmosphere. After 4 h, the DMA conversion reached ≥98% (as judged by ^{1}H NMR), and a degassed mixture of DEA monomer (4.26 g, 23.0 mmol) and 5 mL of MeOH was transferred to the reaction flask via a double-tipped stainless needle. After another 8 h, the polymerization was terminated by exposing the reaction mixture to air and diluting with 10 mL of methanol, leading to the aerial oxidation of the Cu(I) catalyst. The diblock copolymer was purified by being passed through a neutral alumina

Scheme 1. Reaction Schemes for Syntheses of Aldehyde Terminally Functionalized Diblock (*Ald*-PDMA-*b*-PDEA) and Triblock Copolymers (*Ald*-POEGMA-*b*-PDMA-*b*-PDEA)[a]

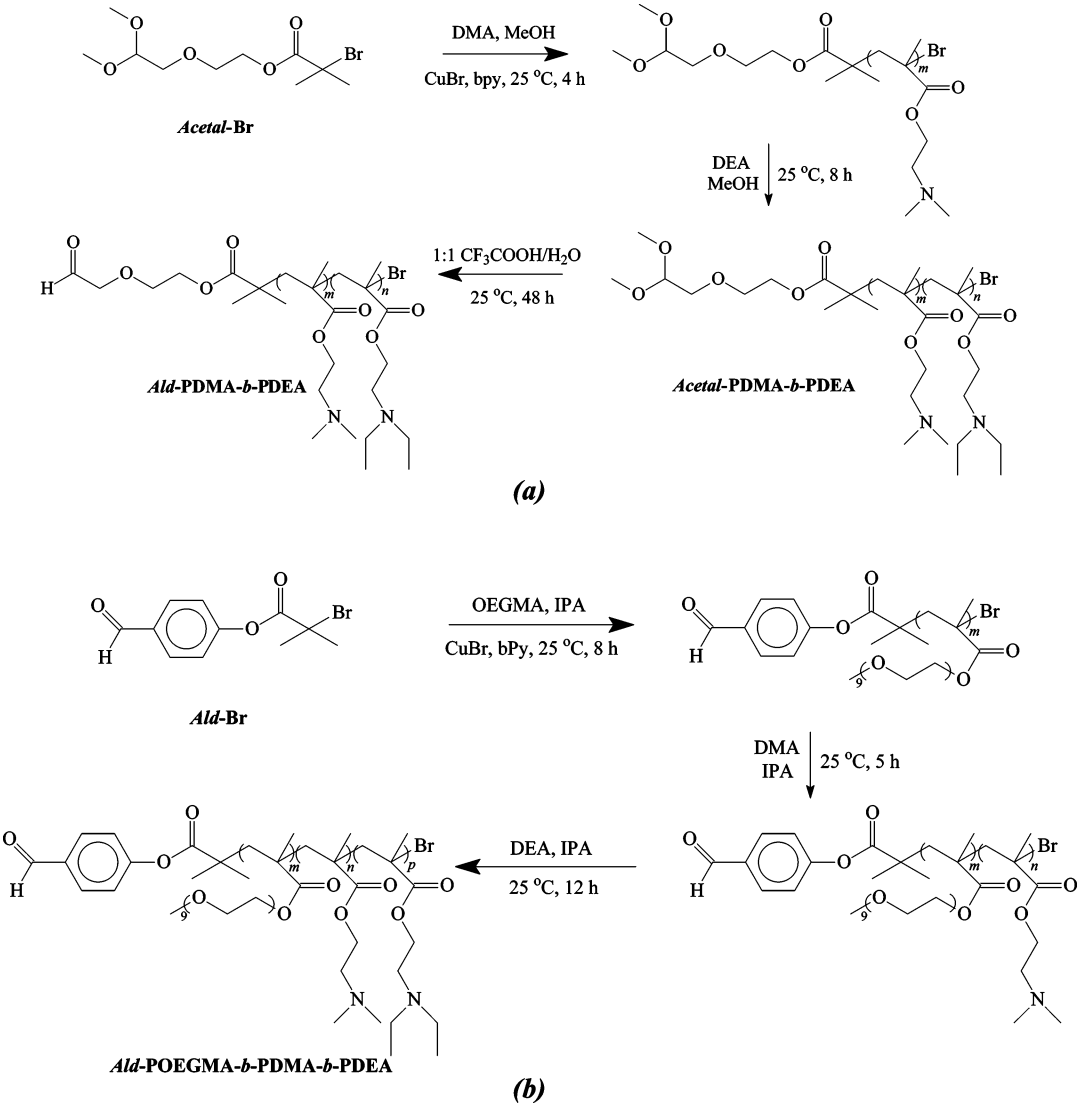

[a] Employed two approaches are shown in panels a and b, respectively.

column to remove the copper catalyst. After evaporating all the solvents, the obtained product was dissolved in THF, precipitated into cold *n*-hexane (−50 °C), and dried in a vacuum oven overnight at room temperature. The overall yield was ∼81%.

For the deprotection of terminal acetal groups, 1.0 g of the obtained acetal-terminated polymer, *Acetal*-PDMA-*b*-PDEA, was dissolved in a 10 mL of 1:1 (v/v) trifluoroacetic acid (TFA)/H_2O mixture, and the solution was stirred at ambient temperature for 48 h. Most of the TFA was removed under reduced pressure, and the polymer was precipitated by adjusting the solution to pH 10−11 with 0.1 M NaOH. The crude product was washed with distilled water several times and dried in a vacuum oven overnight at room temperature. It was then dissolved in THF and precipitated into cold *n*-hexane (−50 °C) to yield the targeted *Ald*-PDMA-*b*-PDEA diblock copolymer.

Synthesis of α-Aldehyde Terminally Functionalized POEGMA-*b*-PDMA-*b*-PDEA Triblock Copolymer (*Ald*-POEGMA-*b*-PDMA-*b*-PDEA). α-Aldehyde terminally functionalized POEGMA-*b*-PDMA-*b*-PDEA triblock copolymer was synthesized by ATRP in a one-pot manner as described next. OEGMA monomer (2.38 g, 5 mmol), *Ald*-Br initiator (0.068 g, 0.25 mmol), bpy (78 mg, 0.5 mmol), and IPA (3 mL) were charged into a round-bottomed flask sealed with a rubber septum, and the solution was then degassed via three freeze−thaw−pump cycles. Upon warming to room temperature, CuBr (0.036 g, 0.25 mmol) was introduced to start the polymerization under nitrogen atmosphere. The reaction solution turned dark brown immediately and became progressively more viscous. After about 8 h, the conversion of OEGMA reached ∼98% (as judged by ^{1}H NMR). A degassed solution of DMA monomer (1.57 g, 10 mmol) in 2 mL of IPA was then introduced into the flask via a double-tipped needle. The reaction mixture turned deeper brown within a few minutes. At the end of the DMA polymerization (∼5 h, ∼98% conversion), a degassed solution of DEA monomer (2.78 g, 15 mmol) in 3 mL of IPA was transferred into the polymerization flask via a double-tipped needle, and the polymerization of the DEA monomer was allowed to proceed overnight. The polymerization was terminated by exposing the reaction solution to air. The blue reaction mixture was then diluted with THF and passed through a column of neutral alumina to remove copper catalysts. After removing the solvents under reduced pressure, the obtained polymer was dissolved in THF and precipitated into cold *n*-hexane (−50 °C) 2 times. After decantation, the residues were dried and then dissolved in THF at a concentration of 2 wt %. The solution was added dropwise into an excess of *n*-hexane at room temperature. The supernatant bluish solution (characteristic of micellar aggregates) was collected. The solvent was removed using a rotary evaporator, and the final product was dried in vacuo overnight at room temperature.

Preparation of Aldehyde Surface-Functionalized SCL Micelles. An aqueous solution of *Ald*-POEGMA-*b*-PDMA-*b*-PDEA

was prepared by molecularly dissolving the copolymer in deionized water at pH 2 and a concentration of 2.0 g/L. Micellization was induced by adjusting to pH 9 with 0.1 M NaOH prior to the addition of BIEE (50 mol % with respect to total DMA residues, corresponding to a target degree of cross-linking of 100%). The aqueous solution was stirred at room temperature for 3 days to ensure effective covalent stabilization of PDEA−core micelles.

Conjugation of Ald-POEGMA-*b*-PDMA-*b*-PDEA or SCL Micelles with Lysozyme. For the conjugation reaction of lysozyme with *Ald*-POEGMA-*b*-PDMA-*b*-PDEA triblock copolymer and SCL micelles, lysozyme (10 mg, 6.8×10^{-7} mol) was dissolved in 100 mL of aqueous solutions of *Ald*-POEGMA-*b*-PDMA-*b*-PDEA or SCL micelles at a copolymer concentration of 2.0 g/L and pH 6.0. The molar ratio of lysozyme to terminal aldehyde groups was ~1:10. The mixed solution was stirred at room temperature for 3 days. In separate experiments, the conjugation was also conducted in the presence of $NaCNBH_3$, which can reduce the formed Schiff bases to stable amino groups. The added $NaCNBH_3$ amount was 1 molar equiv to lysozyme.

Characterization. Nuclear Magnetic Resonance (NMR) Spectroscopy. All ^{1}H NMR analyses were performed at 25 °C on a Bruker AV300 NMR spectrometer (resonance frequency of 300 MHz for ^{1}H) operating in the Fourier transform mode. $CDCl_3$ and D_2O were used as the solvents.

Gel Permeation Chromatography (GPC). Molecular weight distributions were determined by DMF GPC equipped with two Styragel columns (HT3 and HT4) and an oven temperature of 50 °C or THF GPC equipped with a series of three linear Styragel columns (HT2, HT4, and HT5) and an oven temperature of 40 °C. The eluents were at a flow rate of 1.0 mL/min. Waters 1515 pump and Waters 2414 differential refractive index detector (set at 30 °C) were used. A series of six polystyrene standards with molecular weights ranging from 800 to 400 000 g/mol was used for calibration.

Laser Light Scattering (LLS). A commercial spectrometer (ALV/DLS/SLS-5022F) equipped with a multi-τ digital time correlator (ALV5000) and a cylindrical 22 mW UNIPHASE He−Ne laser ($\lambda_0 = 632$ nm) as the light source was employed for dynamic and static LLS measurements at 25 °C. All solutions were clarified by 0.45 μm Millipore nylon filters. In dynamic LLS, scattered light was collected at a fixed angle of 90° for a duration of 15 min. Distribution averages and particle size distributions were computed using cumulants analysis and CONTIN routines. All data were averaged over three measurements.

In static LLS, we can obtain the weight-average molar mass (M_w) and the *z*-average root-mean square radius of gyration ($\langle R_g^2 \rangle^{1/2}$ or written as $\langle R_g \rangle$) of polymer chains or aggregates in a dilute solution from the angular dependence of the excess absolute scattering intensity, known as the Rayleigh ratio $R_{vv}(q)$, as

$$\frac{KC}{R_{vv}(q)} \approx \frac{1}{M_w}\left(1 + \frac{1}{3}\langle R_g^2 \rangle q^2\right) + 2A_2C \qquad (1)$$

where $K = 4\pi^2 n^2 (dn/dC)^2/(N_A \lambda_0^4)$ and $q = (4\pi n/\lambda_0)\sin(\theta/2)$ with N_A, dn/dC, n, and λ_0 being Avogadro's number, the specific refractive index increment, the solvent refractive index, and the wavelength of the laser light in a vacuum, respectively, and A_2 is the second virial coefficient. The specific refractive index increment was determined by a precise differential refractometer. Also note that in this study, the sample solution was so dilute (0.01 g/L) that the extrapolation of $C \rightarrow 0$ was not necessary, and the term $2A_2C$ in eq 1 can be neglected. Thus, the obtained M_w should be considered as apparent values, denoted as $M_{w,app}$.

Transmission Electron Microscopy (TEM). TEM observations were conducted on a Hitachi H-800 electron microscope at an acceleration voltage of 200 kV. The sample for TEM observations was prepared by placing 10 μL of solution on copper grids coated with thin films of Formvar and carbon successively. No staining was required.

Surface Tensiometry. Equilibrium surface tensions were measured using a JK99B tensiometer with a platinum plate. The measuring accuracy of the device as reported by the manufacturer is ±0.1 mN/m. The reported surface tension was the average of four to five measurements that were taken after allowing each of the solutions to equilibrate in the instrument at a temperature of 25.0 ± 0.2 °C.

Gel Electrophoresis. SDS-PAGE was carried out on a gel electrophoresis apparatus (Bio-Rad). Aqueous solutions of the triblock copolymer and the SCL micelles were mixed with SDS, bromophenol blue, glycerol, and 2% β-mercaptoethanol. The 15 wt % and 6 wt % polyacrylamide gels were cast according to standard methods for the gel electrophoresis of lysozyme, lysozyme−triblock copolymer conjugates, and lysozyme−SCL micelle conjugates, respectively. Staining was accomplished with Coomassie Brilliant Blue.

Results and Discussion

Syntheses of α-Aldehyde Terminally Functionalized Block Copolymers. Two approaches were examined for the preparation of aldehyde end-functionalized DHBCs of DMA, DEA, and OEGMA (Scheme 1).

In the first approach, the ATRP initiator (*Acetal*-Br) derived from an aliphatic acetal[78] was employed for the sequential polymerization of DMA and DEA monomers in methanol,[55,56,67] leading to the formation of the *Acetal*-PDMA-*b*-PDEA diblock copolymer. DMF GPC analysis of the resulting diblock copolymer revealed a monomodal and relatively broad elution peak (see Figure S1 in the Supporting Information). The ^{1}H NMR spectrum of *Acetal*-PDMA-*b*-PDEA in $CDCl_3$ is shown in Figure S2 in the Supporting Information. All signals characteristic of the PDMA and PDEA blocks were clearly visible. It should be noted that we can observe a slight resonance signal at 3.6 ppm, which should be ascribed to the -OC*H*$_3$ groups, resulting from the self-catalyzed trans-esterification reaction between ester groups and methanol.[80] The resonance peak due to methyl protons of the terminal acetal groups at $\delta = 3.4$ ppm is clearly visible.

The obtained *Acetal*-PDMA-*b*-PDEA diblock copolymer was converted into *Ald*-PDMA-*b*-PDEA via deprotection in a TFA/water mixture.[78] The deprotected product was collected by precipitation from alkaline solution. Figure S2 in the Supporting Information also shows the ^{1}H NMR spectrum of *Ald*-PDMA-*b*-PDEA in $CDCl_3$. The resonance peak of methyl protons in the terminal acetal groups at 3.4 ppm completely disappeared, accompanied by the appearance of a new peak at ~9.27 ppm corresponding to the terminal aldehyde groups. This indicates the complete deprotection of terminal acetal groups.[78] However, a closer examination of the spectrum tells us that the peak integral ratio of signals characteristic of the aldehyde group with that of tertiary amine residues is quite low, as compared to theoretical values based on the chemical composition of the acetal-terminated diblock copolymer precursor. This indicates that some terminal aldehyde groups were lost during deprotection.

This assumption was further confirmed by the GPC results of the deprotected product (see Figure S1 in the Supporting Information). A bimodal peak was observed; the peak molecular weight of the shoulder at the higher molecular weight side is ca. twice as that of the diblock precursor. The formation of a dimer can be reasonably explained by the aldol condensation reaction between two neighboring chains, leading to the partial disappearance of terminal aldehyde groups.[81] A schematic illustration of the formation of dimers through aldol condensation is shown in Scheme 2.

In the current case, even if the deprotected product can be collected in the protonated form, subsequent pH-induced micellization and SCL need to be conducted in alkaline media,[54−56,58]

Scheme 2. Reaction Schemes for Dimerization of *Ald*-PDMA-*b*-PDEA Diblock Copolymer Chains through Aldol Condensation at Alkaline Conditions

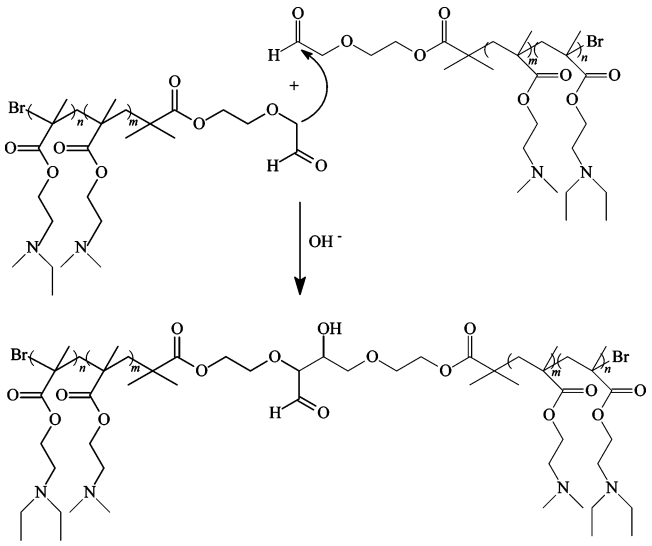

which will still be complicated by possible aldol condensation reactions. On the basis of the previous discussion, we can conclude that the approach starting from the aliphatic acetal-containing ATRP initiator (Scheme 1a) is not suitable for the preparation of aldehyde-terminated DHBCs containing tertiary amine residues.

To avoid an unfavorable aldol condensation reaction due to the presence of terminal aliphatic aldehyde groups, an alternate approach was employed (Scheme 1b).[82] An ATRP initiator, *Ald*-Br,[26,27,79] derived from an aromatic aldehyde that does not contain active protons on the α-carbon was employed for the direct preparation of aldehyde terminally functionalized block copolymers.

On the other hand, it has been shown that ABC triblock copolymers offer significant advantages over AB diblock copolymers for the preparation of SCL micelles due to the avoidance of inter-micelle fusion;[54−56,58] thus, the α-aldehyde terminally functionalized triblock copolymer, *Ald*-POEGMA-*b*-PDMA-*b*-PDEA, can be facilely prepared via sequential ATRP polymerizations of OEGMA, DMA, and DEA in IPA using *Ald*-Br as the initiator. IPA was chosen as the solvent because it can suppress trans-esterification reactions,[80] which has been typically observed when methanol is used as the solvent (Figure S2 in the Supporting Information).

Figure 1 shows the evolution of THF GPC traces during the syntheses of the *Ald*-POEGMA-*b*-PDMA-*b*-PDEA triblock copolymer by sequential ATRP. The GPC trace of the POEGMA precursor just before the addition of the DMA monomer is monomodal, revealing a polydispersity, M_w/M_n, of 1.17. The controlled ATRP of OEGMA has been previously reported.[54,78,83,84] At the end of the polymerization of DMA, samples were withdrawn for GPC analysis. We can clearly observe the shift to higher molecular weight after the chain extension with the PDMA block. There is no tailing at the lower molecular weight side, indicating that the initiating efficiency of the POEGMA macroinitiator for the ATRP of DMA is quite high. However, we can discern a slight shoulder at the high molecular weight side, which can be attributed to biradical termination reactions.

The polymerization of the DEA monomer was conducted for 12 h. After passing through a neutral alumina column and removing all the solvent, the residues were further purified to

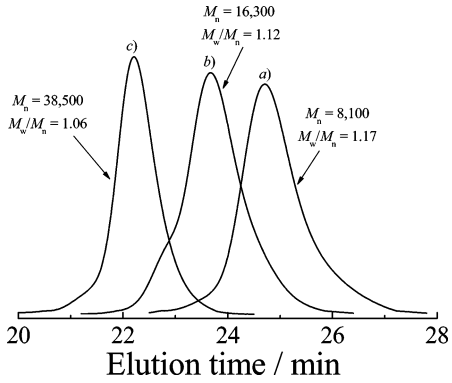

Figure 1. Evolution of THF GPC traces during the synthesis of *Ald*-POEGMA-*b*-PDMA-*b*-PDEA triblock copolymer: (a) 8 h after polymerization of POEGMA block, just before the addition of DMA monomer; (b) 5 h after addition of DMA monomer, just before addition of DEA monomer; and (c) final POEGMA-*b*-PDMA-*b*-PDEA triblock copolymer after purification.

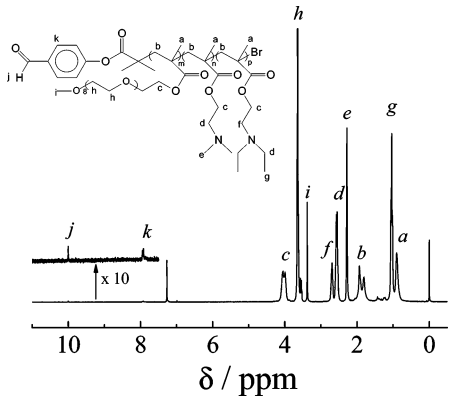

Figure 2. ^{1}H NMR spectrum of *Ald*-POEGMA$_{22}$-*b*-PDMA$_{48}$-*b*-PDEA$_{78}$ triblock copolymer in $CDCl_3$.

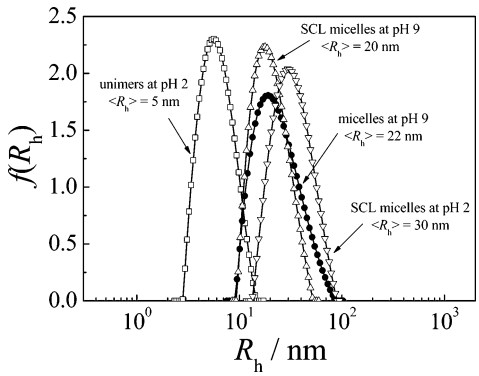

Figure 3. Hydrodynamic radius distributions, $f(R_h)$, obtained for 2.0 g/L aqueous solution of *Ald*-POEGMA$_{22}$-*b*-PDMA$_{48}$-*b*-PDEA$_{78}$ triblock copolymer at 25 °C: unimers at pH 2 (□), micelles at pH 9 (●), SCL micelles at pH 9 (△), and SCL micelles at pH 2 (▽). The target degree of cross-linking was 100%.

remove residual monomers and terminated *Ald*-POEGMA-*b*-PDMA chains. A GPC trace of the purified product is shown in Figure 1, revealing a monomodal and symmetric peak, with an M_n of 38 500 and a polydispersity, M_w/M_n, of 1.06. The shift to the higher molecular weight side as compared to that of the diblock copolymer precursor is clearly evident.

The ^{1}H NMR spectrum of the obtained *Ald*-POEGMA-*b*-PDMA-*b*-PDEA triblock copolymer in $CDCl_3$ is shown in Figure 2, together with the peak assignments. All signals characteristic of POEGMA, PDMA, and PDEA blocks are clearly visible. Most importantly, the resonance peak due to the terminal aldehyde groups at $\delta = 10.0$ ppm can be clearly

Scheme 3. Schematic Illustration of Preparation of Aldehyde Surface-Functionalized SCL Micelles and Their Subsequent Bioconjugation with Lysozyme via Formation of Schiff Bases

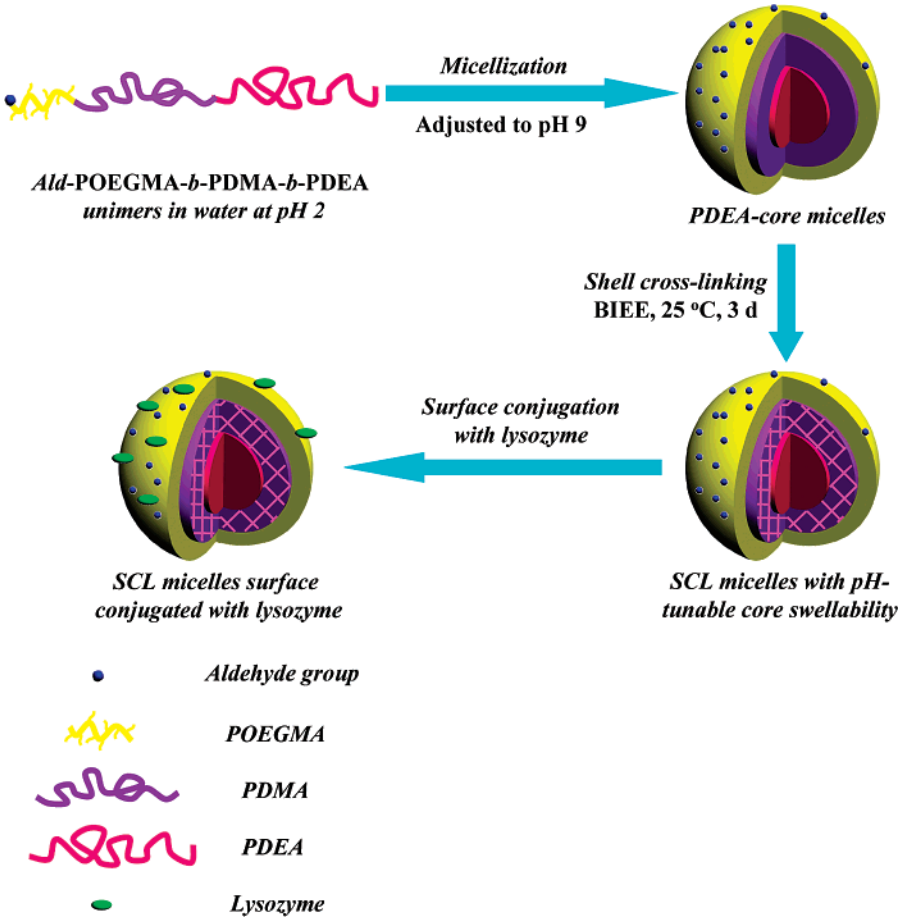

observed. The actual degrees of polymerization, DP, of the POEGMA, PDMA, and PDEA blocks were calculated to be 22, 48, and 78, respectively, based on the integral ratios of the terminal aldehyde signal to those characteristic of each block. Thus, the triblock copolymer was denoted as *Ald*-POEGMA$_{22}$-*b*-PDMA$_{48}$-*b*-PDEA$_{78}$.

Aldehyde Surface-Functionalized SCL Micelles. The PDMA and PDEA homopolymers are both weak polybases with pK_a values of 7.1 and 7.3, respectively.[85−88] The PDMA homopolymer is water-soluble over a wide pH range with a slightly lower solubility at pH > 9−10. In contrast, the PDEA homopolymer is water-insoluble at neutral or alkaline pH. Below pH 6, it is soluble as a weak cationic polyelectrolyte due to protonation of tertiary amine residues. Thus, similar to the previously reported micellization behavior of PEO-*b*-PDMA-*b*-PDEA,[56,67] the *Ald*-POEGMA-*b*-PDMA-*b*-PDEA triblock copolymer will also form three-layer onion-like micelles consisting of a PDEA core, a PDMA inner shell, and a biocompatible POEGMA outer corona. Most importantly, the surface of the micelles was functionalized with reactive aldehyde groups (Scheme 3). This was further confirmed by subsequent LLS and ^{1}H NMR studies.

Figure 3 shows dynamic LLS results of the *Ald*-POEGMA$_{22}$-*b*-PDMA$_{48}$-*b*-PDEA$_{78}$ triblock copolymer at a concentration of 2.0 g/L. At pH 2, the triblock copolymer molecularly dissolves, with an intensity-average hydrodynamic radius, $\langle R_h \rangle$, of approximately 5−6 nm and very low scattered intensity. Upon a pH increase to 9, micellization occurs as indicated by the bluish tinge characteristic of micellar solutions. Dynamic LLS revealed only one population, with a $\langle R_h \rangle$ of 22 nm. As the PDEA block is becoming water-insoluble at pH 9, dynamic LLS results suggest the formation of micelles with PDEA cores.[56] Moreover, the formed micelles are nearly monodisperse, with a polydispersity index, μ_2/Γ^2, of 0.11.

As chain segments in the micelle core possess decreased mobility as compared to that of free chains in solution, ^{1}H NMR spectroscopy can be conveniently utilized to study the micellization of stimuli-responsive block copolymers, providing the structural information of which block sequence in the copolymer is forming the micellar core. Figure 4 shows the ^{1}H NMR spectra of the *Ald*-POEGMA$_{22}$-*b*-PDMA$_{48}$-*b*-PDEA$_{78}$ triblock copolymer in D_2O at different pH. At pH 2, the copolymer chains are fully solvated, and all the signals expected for each block are visible. At pH 9, the signal characteristic of PDEA block at δ = 1.4 ppm completely disappear, while the signals from the POEGMA and PDMA blocks are clearly visible, indicating the formation of three-layer onion-like micelles with PDEA cores, PDMA inner layers, and POEGMA outer coronas (Scheme 3). Most importantly, the resonance peak due to the terminal aldehyde groups was also clearly visible at ca. 10.0 ppm. This indicates that the formed micelles were surface-functionalized with aldehyde groups.

The micellization behavior of the *Ald*-POEGMA$_{22}$-*b*-PDMA$_{48}$-*b*-PDEA$_{78}$ triblock copolymer in aqueous solution was also studied by surface tensiometry.[85,87,88] The variation of surface tension with solution pH obtained for the triblock copolymer at a constant polymer concentration of 2.0 g/L is shown in Figure 5a. Below pH 6, this triblock copolymer molecularly dissolved with a relatively high surface tension value (~57 mN/m). Upon further increasing solution pH, the triblock copolymer became significantly more surface active, due to that the PDEA

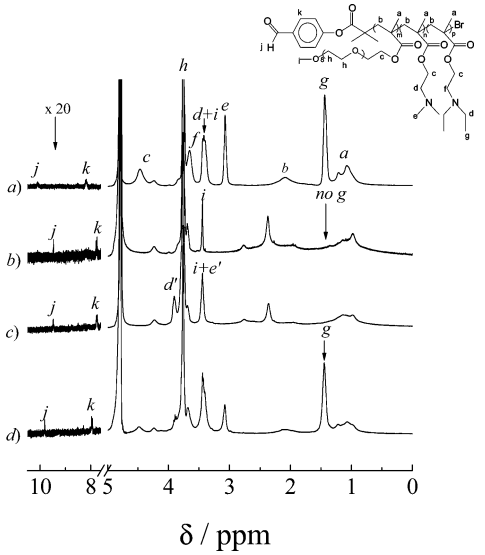

Figure 4. ^{1}H NMR spectra of *Ald*-POEGMA$_{22}$-*b*-PDMA$_{48}$-*b*-PDEA$_{78}$ triblock copolymer at 10 g/L in D_2O: (a) at pH 2; (b) at pH 9; (c) after SCL, at pH 9; and (d) after SCL, at pH 2. The target degree of cross-linking was 100%.

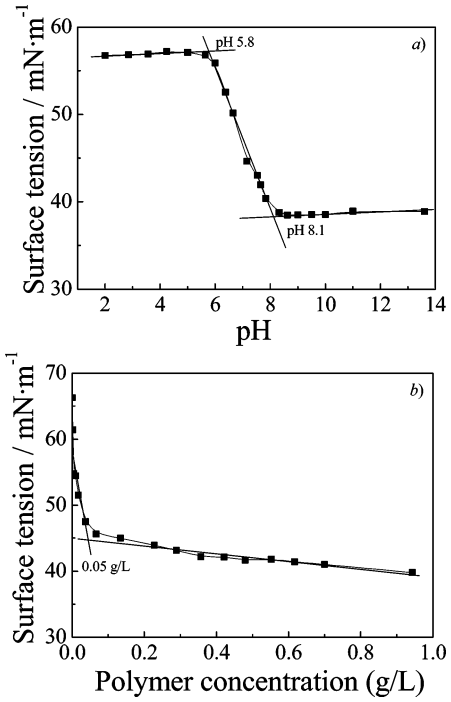

Figure 5. (a) Variation of surface tension with solution pH at a constant *Ald*-POEGMA$_{22}$-*b*-PDMA$_{48}$-*b*-PDEA$_{78}$ concentration of 2.0 g/L. (b) Variation of surface tension with the *Ald*-POEGMA$_{22}$-*b*-PDMA$_{48}$-*b*-PDEA$_{78}$ concentrations at a fixed pH of 9.0.

block was becoming deprotonated and more hydrophobic. It will then adsorb strongly at the air−water interface and also form the dehydrated micelle cores, leading to the reduction of surface tension values. Above pH 8, the limiting surface tension of the triblock copolymer solution was reached, remaining at a constant value of ∼39 mN/m. The data shown in Figure 5a also told us that the most dramatic decrease of surface tension occurred within the narrow pH range of 6−8; this agrees quite well with the reported pK_a value of the PDEA block (∼7.3).[85−88]

We also identified the cmc from the concentration dependence of surface tensions of the triblock copolymer in aqueous solution (Figure 5b).[87] The cmc of the triblock copolymer in aqueous solution was estimated to be 0.05 g/L, as indicated by the inflection point of the surface tension versus concentration curve. Below the cmc, triblock copolymer micelles will dissociate into unimers. If this novel type of DHBC micelles possessing pH-responsive cores is to be employed as drug nanocarriers, the drug-loaded micelles will inevitably dissociate into unimers after administration.

To solve this problem, the block copolymer micelles can be SCL to stabilize their nanostructure, while keeping the pH-responsive cores for the ability of encapsulating drug molecules. The SCL of DHBC micelles has been extensively investigated by Armes and co-workers.[53−60] In the current case, the PDMA inner shell can be facilely cross-linked with BIEE, which can selectively quaternize the PDMA blocks on adjacent copolymer chains to lock in the micellar structure (Scheme 3).[53−56,58,88]

The obtained SCL micelles were studied in detail employing a combination of techniques, such as LLS, ^{1}H NMR, and TEM. Dynamic LLS reveals a $\langle R_h \rangle$ of 20 nm for SCL micelles at pH 9 (Figure 3), which is slightly smaller than that before SCL.[56] For SCL micelles, the bluish tinge can persist upon adjusting the solution to pH 2. Most importantly, the scattered intensity remained almost the same as that at pH 9. This strongly suggests that SCL has successfully fixed the micellar structure. Otherwise, the micelles will dissociate into unimers at acidic pH, leading to a large decrease of scattered light intensity.[56]

Typical ^{1}H NMR spectra of aqueous solutions of SCL micelles in D_2O are shown in Figure 4. For the SCL micelles at pH 9 (Figure 4c), the signals due to the DMA residues at $\delta = 2.4$ and 2.8 ppm are still evident. Comparing the signals due to unquaternized DMA residues at $\delta = 2.4$ ppm to that due to the OEGMA block at $\delta = 3.7$ ppm allows the estimation of actual degree of quaternization, which is ∼65%. The target degree of quaternization sets a high limit for the actual degree of cross-linking.[56] Upon adjusting the solution to pH 2 using DCl, the characteristic PDEA signals at $\delta = 1.4$ ppm reappear, indicating that the PDEA−core is becoming hydrophilic and swollen (Figure 4d).[56]

At pH 2, dynamic LLS reveals a $\langle R_h \rangle$ of ∼30 nm for the SCL micelles, suggesting that the PDEA−core of SCL micelles can swell (Figure 3). Upon adjusting the solution pH from 9 to 2, the swelling of the PDEA−core leads to a 3.4-fold increase of the hydrodynamic volume of SCL micelles (Scheme 3). As the three-layer core−shell−corona microstructure of the obtained SCL micelles is fixed due to cross-linking of the inner PDMA shell, static LLS can be conducted at a quite low concentration (0.01 g/L).

The angular dependence of the Rayleigh ratio, $R_{vv}(q)$, obtained at a concentration of 0.01 g/L, leads to the determination of an average radius of gyration, $\langle R_g \rangle$, and an apparent weight-average molar mass, $M_{w,app}$, of SCL micelles (see Figure 6). $\langle R_g \rangle$ values of the SCL micelles were determined to be 16 and 29 nm at pH 9 and 2, respectively. Moreover, the $\langle R_g \rangle / \langle R_h \rangle$ ratio at pH 2 (0.97) is larger than that at pH 9 (0.80). Thus, static LLS results can further confirm the swelling of PDEA cores of SCL micelles at low pH, leading to more uniform distribution of chain densities within nanoparticles.

$M_{w,app}$ values of the SCL micelles are 2.8×10^6 and 2.9×10^6 g/mol at pH 9 and 2, respectively. The almost constant $M_{w,app}$ at two different pH values suggests the successful locking of the micellar structure after SCL. The average densities of the SCL micelles at pH 9 and 2 were calculated to be 0.14 and 0.043 g/cm^3. The much lower micelle density at pH 2 also suggests extensive swelling of the PDEA cores due to complete protonation of tertiary amine residues. The average aggregation number, N_{agg}, of the obtained SCL micelles is calculated to be

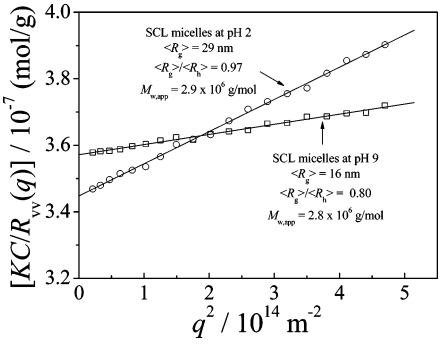

Figure 6. Angular dependence of the Rayleigh ratio, $R_{vv}(q)$, of SCL micelles in aqueous solutions at two different pH values measured by static LLS over the scattering angle range of 20−110°.

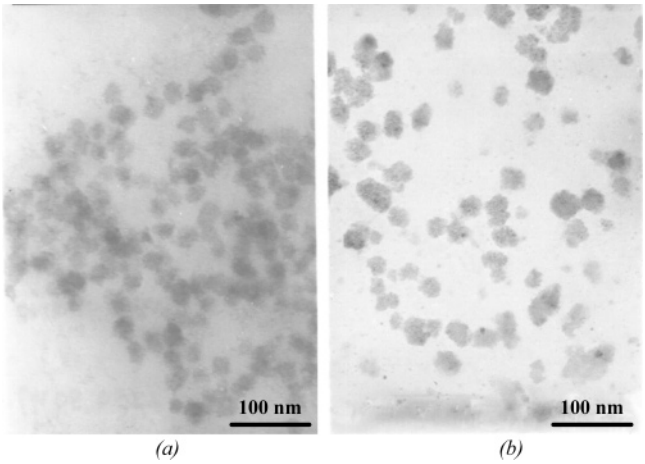

Figure 7. Typical TEM images of SCL micelles of *Ald*-$POEGMA_{22}$-*b*-$PDMA_{48}$-*b*- $PDEA_{78}$ triblock copolymer at pH 9 (a) and pH 2 (b). The target degree of cross-linking was 100%.

∼80. As the aldehyde group is attached at the POEGMA chain end, on average, there are ∼80 aldehyde groups at the surface of one SCL micelle.

TEM observations were further performed on solutions of SCL micelles to examine their structures. Typical TEM images are shown in Figure 7, revealing the presence of nearly monodisperse and spherical nanoparticles. On average, the particles sizes were ∼20 and ∼25 nm in diameter for SCL micelles at pH 9 and 2, respectively, which are quite comparable to the micelle dimensions obtained from dynamic LLS studies (Figure 3).

Conjugation of Aldehyde-Functionalized Triblock Copolymer or SCL Micelles with Lysozyme. For SCL micelles fabricated from *Ald*-POEGMA-*b*-PDMA-*b*-PDEA, the presence of surface aldehyde groups is clearly evident, as indicated by the resonance signal at ca. 10.0 ppm (Figure 4d). Theoretically, the SCL micelles can act as multi-functional drug nanocarriers possessing the following four main advantages (Scheme 3). First, covalent stabilization for the polymeric micelles is achieved by SCL of the PDMA inner shell, which should lead to high circulation stability in the blood compartments; second, the reversible pH-sensitive swelling/deswelling of the PDEA core of SCL micelles enables the encapsulation of hydrophobic drugs and the subsequent controlled release; third, the POEGMA blocks in the corona are completely biocompatible and nontoxic, which can avoid recognition of the nanocarriers by the reticuloendothelial system and nonspecific deposition after administration; and finally, the reactive aldehyde groups at the surface of SCL micelles allow for their facile conjugation with bioactive pilot molecules such as peptide,[12−16] protein, folate,[17−20] saccharide,[21−24] and DNA sequences,[35,52] achieving targeted delivery and preferential accumulation at the designated area.

As a proof-of-concept demonstration, we chose a commercially available protein, lysozyme, as a model protein for its bioconjugation with SCL micelles via the formation of Schiff bases (Scheme 3). Lysozyme has seven free amino groups, and the bioconjugation reactions are carried out in phosphate buffer at pH 6.0 in the presence or absence of $NaCNBH_3$, which can in situ reduce the formed Schiff bases into amines.[15,16,78] The molar ratios of lysozyme to aldehyde groups of triblock copolymers or SCL micelles were fixed at 1:10 in all cases. SDS-PAGE results of free lysozyme and triblock copolymer−protein bioconjugates are shown in Figure 8a−c. As compared to the electrophoresis band of free lysozyme (Figure 8a), the bands of the bioconjugates prepared in the presence or absence of $NaCNBH_3$ (Figure 8b,c) move much more slowly during electrophoresis, apparently indicating much higher molecular weights. Most importantly, both of the latter two bands clearly reveal the absence of free lysozyme, suggesting that all lysozyme molecules are conjugated to the triblock copolymers. This is reasonable considering that the amount of terminal aldehyde groups is in large excess relative to that of lysozyme.

It should be noted that the bands of triblock copolymer−protein conjugates are relatively broad, probably due to the relatively polydisperse nature of copolymer chains as compared to that of protein, which possesses a uniform molecular weight and chemical structure. There exist no discernible differences between the conjugates prepared in the presence or absence of $NaCNBH_3$. Actually, the Schiff bases formed between aromatic aldehydes and primary amines are quite stable,[89,90] which is different from that formed between aliphatic aldehyde and primary amine as reported by Haddleton et al.[78] In the latter case, in situ reduction of the newly formed Schiff bases with $NaCNBH_3$ is necessary to avoid their transformation back into original aldehydes and primary amines.

As compared to the band of free lysozyme (Figure 8d), the SDS-PAGE trace of SCL micelle−lysozyme conjugates clearly revealed the absence of bands due to free lysozyme (Figure 8e). This indicates that all lysozyme molecules were covalently conjugated to the surface of SCL micelles. Under the electrophoresis conditions (15 wt % polyacrylamide gel, 2 h electrophoresis time), the SDS-PAGE trace did not reveal the presence of SCL micelle−protein bioconjugates, probably due to that the bioconjugates possess quite high molar masses (∼3 × 10^6 g/mol). However, we can still discern a slightly shaded band in the molecular weight range of 40−50 kDa, as indicated by the marker bands, which should be ascribed to lysozyme conjugates with unimer chains. As the PDEA−core micelles formed in alkaline pH are always in equilibrium with unimers possessing a concentration of cmc, both SCL micelles and unimers will coexist in solution. However, these unimers can be facilely removed via dialysis against water before conjugation, leading to SCL micelle dispersions free of unimer chains.

Under an alternate electrophoresis condition (6 wt % polyacrylamide gel, 12 h electrophoresis time), we can clearly see the band due to bioconjugates of SCL micelles and lysozyme. The molar ratio of lysozyme molecules to that of surface aldehyde groups of SCL micelles was 1:10, and there are ∼80 surface aldehyde groups per SCL micelle on the basis of static LLS results. Thus, on average, ∼8 lysozyme molecules can be conjugated at the surface of one SCL micelle. It should be noted that there are still residual aldehyde groups at the surface of bioconjugates of SCL micelles and lysozymes, which can allow for further functionalization with other bioactive moieties.[12,13,49]

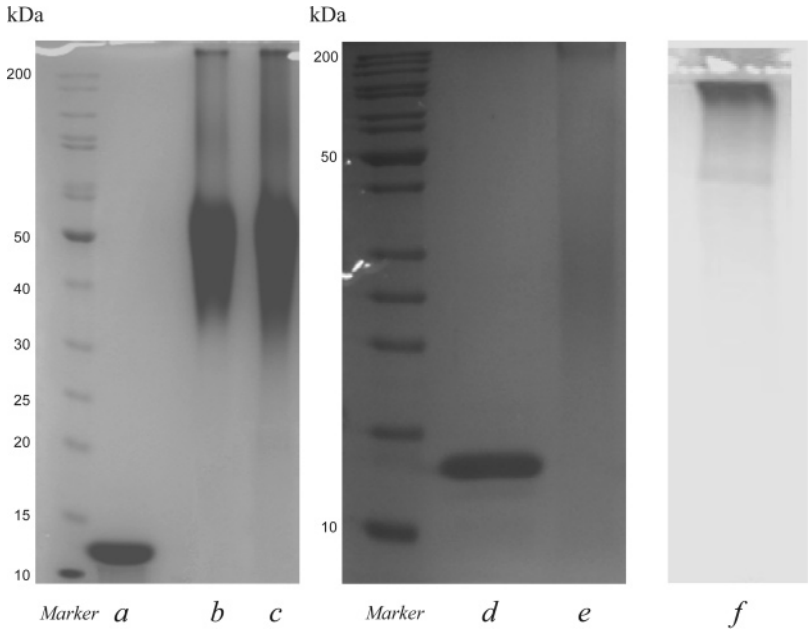

Figure 8. SDS-PAGE traces obtained for bioconjugates of lysozyme with *Ald*-POEGMA$_{22}$-*b*-PDMA$_{48}$-*b*-PDEA$_{78}$ triblock copolymer and SCL micelles: (a) free lysozyme; (b) lysozyme-triblock copolymer bioconjugate prepared in the absence of $NaCNBH_3$; (c) lysozyme-triblock copolymer bioconjugate prepared in the presence of $NaCNBH_3$; and (e and f) bioconjugates of SCL micelles and lysozyme. The polyacrylamide gels used in lanes a−e were 15 wt %, and the time of electrophoresis was 2 h, while that used in lane f was 6 wt %, and the time of electrophoresis was 12 h.

Conclusion

α-Aldehyde terminally functionalized double hydrophilic triblock copolymer, *Ald*-POEGMA-*b*-PDMA-*b*-PDEA, was successfully synthesized via sequential ATRP of OEGMA, DMA, and DEA monomers using an aromatic aldehyde-containing initiator. The triblock copolymer molecularly dissolves in acidic media and can self-assemble at alkaline pH into three-layer onion-like micelles consisting of a pH-sensitive PDEA core, a cross-linkable PDMA inner layer, and a biocompatible POEGMA outer corona. Most importantly, the surface of micelles was functionalized with reactive aldehyde groups. SCL of the PDMA inner layer led to structurally stable SCL micelles. The obtained SCL micelles possessed pH-responsive PDEA cores, which might be utilized for the encapsulation of hydrophobic drugs and subsequent controlled release. The bioconjugation between SCL micelles and model protein, lysozyme, can be facilely conducted at slightly acidic media in the absence of a reducing agent, as evidenced by SDS-PAGE results. This suggests that other bioactive molecules including peptides (e.g., RGD), DNA sequences, and folate can be conveniently conjugated to the surface of SCL micelles under similar conditions to allow for targeted drug delivery.

The reported novel SCL micelles possessing reactive aldehyde groups might act as excellent drug nanocarriers mainly due to four distinct advantages: structural stability resulting from SCL, pH-tunable core swelling/shrinkage for controlled release of encapsulated guest molecules, biocompatibility and nontoxicity of POEGMA outer corona, and versatility of surface bioconjugation due to the presence of reactive aldehyde groups at the periphery, enabling targeted drug delivery and preferential accumulation.

Acknowledgment. This work was financially supported by an Outstanding Youth Fund (50425310) and research grants (20534020 and 20674079) from the National Natural Scientific Foundation of China (NNSFC), the "Bai Ren" Project and Special Grant (KJC 2-SW-H14) of the Chinese Academy of Sciences, and the Program for Changjiang Scholars and Innovative Research Team in University (PCSIRT).

Supporting Information Available: DMF GPC traces and ^{1}H NMR results of *Acetal*-PDMA-*b*-PDEA and *Ald*-PDMA-*b*-PDEA. This information is available free of charge via the Internet at http://pubs.acs.org.

References and Notes

(1) Allen, C.; Maysinger, D.; Eisenberg, A. *Colloids Surf., B* **1999**, *16*, 3.
(2) Gaucher, G.; Dufresne, M. H.; Sant, V. P.; Kang, N.; Maysinger, D.; Leroux, J. C. *J. Controlled Release* **2005**, *109*, 169.
(3) Kabanov, A. V.; Alakhov, V. Y. *Crit. Rev. Ther. Drug Carrier Syst.* **2002**, *19*, 1.
(4) Kabanov, A. V.; Batrakova, E. V.; Alakhov, V. Y. *J. Controlled Release* **2002**, *82*, 189.
(5) Kabanov, A. V.; Batrakova, E. V.; Meliknubarov, N. S.; Fedoseev, N. A.; Dorodnich, T. Y.; Alakhov, V. Y.; Chekhonin, V. P.; Nazarova, I. R.; Kabanov, V. A. *J. Controlled Release* **1992**, *22*, 141.
(6) Kabanov, A. V.; Lemieux, P.; Vinogradov, S.; Alakhov, V. *Adv. Drug Delivery Rev.* **2002**, *54*, 223.
(7) Kataoka, K.; Harada, A.; Nagasaki, Y. *Adv. Drug Delivery Rev.* **2001**, *47*, 113.
(8) Kwon, G. S.; Kataoka, K. *Adv. Drug Delivery Rev.* **1995**, *16*, 295.
(9) Zhang, L. F.; Eisenberg, A. *Science (Washington, DC, U.S.)* **1995**, *268*, 1728.
(10) Zhang, L. F.; Eisenberg, A. *J. Am. Chem. Soc.* **1996**, *118*, 3168.
(11) Discher, D. E.; Eisenberg, A. *Science (Washington, DC, U.S.)* **2002**, *297*, 967.
(12) Liu, J. Q.; Zhang, Q.; Remsen, E. E.; Wooley, K. L. *Biomacromolecules* **2001**, *2*, 362.
(13) Becker, M. L.; Remsen, E. E.; Pan, D.; Wooley, K. L. *Bioconjugate Chem.* **2004**, *15*, 699.
(14) Becker, M. L.; Liu, J. Q.; Wooley, K. L. *Biomacromolecules* **2005**, *6*, 220.
(15) Yamamoto, Y.; Nagasaki, Y.; Kato, M.; Kataoka, K. *Colloids Surf., B* **1999**, *16*, 135.
(16) Yamamoto, Y.; Nagasaki, Y.; Kato, Y.; Sugiyama, Y.; Kataoka, K. *J. Controlled Release* **2001**, *77*, 27.
(17) Licciardi, M.; Giammona, G.; Du, J. Z.; Armes, S. P.; Tang, Y. Q.; Lewis, A. L. *Polymer* **2006**, *47*, 2946.
(18) Licciardi, M.; Tang, Y.; Billingham, N. C.; Armes, S. P. *Biomacromolecules* **2005**, *6*, 1085.
(19) Pan, D.; Turner, J. L.; Wooley, K. L. *Chem. Commun.* **2003**, 2400.
(20) Bae, Y.; Jang, W. D.; Nishiyama, N.; Fukushima, S.; Kataoka, K. *Mol. Biosyst.* **2005**, *1*, 242.
(21) Joralemon, M. J.; Murthy, K. S.; Remsen, E. E.; Becker, M. L.; Wooley, K. L. *Biomacromolecules* **2004**, *5*, 903.
(22) Wakebayashi, D.; Nishiyama, N.; Yamasaki, Y.; Itaka, K.; Kanayama, N.; Harada, A.; Nagasaki, Y.; Kataoka, K. *J. Controlled Release* **2004**, *95*, 653.

(23) Yasugi, K.; Nakamura, T.; Nagasaki, Y.; Kato, M.; Kataoka, K. *Macromolecules* **1999**, *32*, 8024.
(24) Oishi, M.; Nagasaki, Y.; Itaka, K.; Nishiyama, N.; Kataoka, K. *J. Am. Chem. Soc.* **2005**, *127*, 1624.
(25) Iijima, M.; Nagasaki, Y.; Okada, T.; Kato, M.; Kataoka, K. *Macromolecules* **1999**, *32*, 1140.
(26) Narain, R.; Armes, S. P. *Macromolecules* **2003**, *36*, 4675.
(27) Narain, R.; Armes, S. P. *Biomacromolecules* **2003**, *4*, 1746.
(28) Ishii, T.; Otsuka, H.; Kataoka, K.; Nagasaki, Y. *Langmuir* **2004**, *20*, 561.
(29) Kataoka, K.; Harada, A.; Wakebayashi, D.; Nagasaki, Y. *Macromolecules* **1999**, *32*, 6892.
(30) Nagasaki, Y.; Okada, T.; Scholz, C.; Iijima, M.; Kato, M.; Kataoka, K. *Macromolecules* **1998**, *31*, 1473.
(31) Akiyama, Y.; Harada, A.; Nagasaki, Y.; Kataoka, K. *Macromolecules* **2000**, *33*, 5841.
(32) Rheingans, O.; Hugenberg, N.; Harris, J. R.; Fischer, K.; Maskos, M. *Macromolecules* **2000**, *33*, 4780.
(33) Zhang, Q.; Remsen, E. E.; Wooley, K. L. *J. Am. Chem. Soc.* **2000**, *122*, 3642.
(34) Joralemon, M. J.; O'Reilly, R. K.; Hawker, C. J.; Wooley, K. L. *J. Am. Chem. Soc.* **2005**, *127*, 16892.
(35) Thurmond, K. B.; Remsen, E. E.; Kowalewski, T.; Wooley, K. L. *Nucleic Acids Res.* **1999**, *27*, 2966.
(36) Guo, A.; Liu, G. J.; Tao, J. *Macromolecules* **1996**, *29*, 2487.
(37) Henselwood, F.; Liu, G. J. *Macromolecules* **1997**, *30*, 488.
(38) Tao, J.; Liu, G. J.; Ding, J. F.; Yang, M. L. *Macromolecules* **1997**, *30*, 4084.
(39) Kakizawa, Y.; Harada, A.; Kataoka, K. *J. Am. Chem. Soc.* **1999**, *121*, 11247.
(40) Bronich, T. K.; Keifer, P. A.; Shlyakhtenko, L. S.; Kabanov, A. V. *J. Am. Chem. Soc.* **2005**, *127*, 8236.
(41) Zeng, Y.; Pitt, W. G. *J. Biomater. Sci., Polymer Ed.* **2005**, *16*, 371.
(42) Huang, H. Y.; Hoogenboom, R.; Leenen, M. A. M.; Guillet, P.; Jonas, A. M.; Schubert, U. S.; Gohy, J. F. *J. Am. Chem. Soc.* **2006**, *128*, 3784.
(43) O'Reilly, R. K.; Joralemon, M. J.; Hawker, C. J.; Wooley, K. L. *New J. Chem.* **2007**, *31*, 718.
(44) Thurmond, K. B.; Kowalewski, T.; Wooley, K. L. *J. Am. Chem. Soc.* **1996**, *118*, 7239.
(45) Huang, H. Y.; Kowalewski, T.; Remsen, E. E.; Gertzmann, R.; Wooley, K. L. *J. Am. Chem. Soc.* **1997**, *119*, 11653.
(46) Thurmond, K. B.; Kowalewski, T.; Wooley, K. L. *J. Am. Chem. Soc.* **1997**, *119*, 6656.
(47) Huang, H. Y.; Remsen, E. E.; Kowalewski, T.; Wooley, K. L. *J. Am. Chem. Soc.* **1999**, *121*, 3805.
(48) Qi, K.; Ma, Q. G.; Remsen, E. E.; Clark, C. G.; Wooley, K. L. *J. Am. Chem. Soc.* **2004**, *126*, 6599.
(49) Pan, D. J.; Turner, J. L.; Wooley, K. L. *Macromolecules* **2004**, *37*, 7109.
(50) Sun, X. K.; Rossin, R.; Turner, J. L.; Becker, M. L.; Joralemon, M. J.; Welch, M. J.; Wooley, K. L. *Biomacromolecules* **2005**, *6*, 2541.
(51) Joralemon, M. J.; Smith, N. L.; Holowka, D.; Baird, B.; Wooley, K. L. *Bioconjugate Chem.* **2005**, *16*, 1246.
(52) Turner, J. L.; Becker, M. L.; Li, X. X.; Taylor, J. S. A.; Wooley, K. L. *Soft Matter* **2005**, *1*, 69.
(53) Butun, V.; Billingham, N. C.; Armes, S. P. *J. Am. Chem. Soc.* **1998**, *120*, 12135.
(54) Butun, V.; Wang, X. S.; Banez, M. V. D.; Robinson, K. L.; Billingham, N. C.; Armes, S. P.; Tuzar, Z. *Macromolecules* **2000**, *33*, 1.
(55) Liu, S. Y.; Armes, S. P. *J. Am. Chem. Soc.* **2001**, *123*, 9910.
(56) Liu, S. Y.; Weaver, J. V. M.; Tang, Y. Q.; Billingham, N. C.; Armes, S. P.; Tribe, K. *Macromolecules* **2002**, *35*, 6121.
(57) Fujii, S.; Cai, Y. L.; Weaver, J. V. M.; Armes, S. P. *J. Am. Chem. Soc.* **2005**, *127*, 7304.
(58) Pilon, L. N.; Armes, S. P.; Findlay, P.; Rannard, S. P. *Langmuir* **2005**, *21*, 3808.
(59) Jiang, X. Z.; Luo, S. Z.; Armes, S. P.; Shi, W. F.; Liu, S. Y. *Macromolecules* **2006**, *39*, 5987.
(60) Li, Y. T.; Lokitz, B. S.; Armes, S. P.; McCormick, C. L. *Macromolecules* **2006**, *39*, 2726.
(61) André, X.; Zhang, M. F.; Müller, A. H. E. *Macromol. Rapid Commun.* **2005**, *26*, 558.
(62) Bo, Q.; Zhao, Y. *J. Polym. Sci., Part A: Polym. Chem.* **2006**, *44*, 1734.
(63) Schilli, C. M.; Zhang, M.; Rizzardo, E.; Thang, S. H.; Chong, Y. K.; Edwards, K.; Karlsson, G.; Müller, A. H. E. *Macromolecules* **2004**, *37*, 7861.
(64) Mountrichas, G.; Pispas, S. *Macromolecules* **2006**, *39*, 4767.
(65) Liu, S. Y.; Armes, S. P. *Angew. Chem., Int. Ed.* **2002**, *41*, 1413.
(66) Ma, Y. H.; Tang, Y. Q.; Billingham, N. C.; Armes, S. P.; Lewis, A. L.; Lloyd, A. W.; Salvage, J. P. *Macromolecules* **2003**, *36*, 3475.
(67) Tang, Y. Q.; Liu, S. Y.; Armes, S. P.; Billingham, N. C. *Biomacromolecules* **2003**, *4*, 1636.
(68) Zhu, Z. Y.; Armes, S. P.; Liu, S. Y. *Macromolecules* **2005**, *38*, 9803.
(69) Zhang, W.; Shi, L.; Ma, R.; An, Y.; Xu, Y.; Wu, K. *Macromolecules* **2005**, *38*, 8850.
(70) Liu, S. Y.; Armes, S. P. *Langmuir* **2003**, *19*, 4432.
(71) Munoz-Bonilla, A.; Fernandez-Garcia, M.; Haddleton, D. M. *Soft Matter* **2007**, *3*, 725.
(72) Butun, V.; Billingham, N. C.; Armes, S. P. *J. Am. Chem. Soc.* **1998**, *120*, 11818.
(73) Butun, V.; Armes, S. P.; Billingham, N. C.; Tuzar, Z.; Rankin, A.; Eastoe, J.; Heenan, R. K. *Macromolecules* **2001**, *34*, 1503.
(74) Liu, S. Y.; Billingham, N. C.; Armes, S. P. *Angew. Chem., Int. Ed.* **2001**, *40*, 2328.
(75) Arotçaréna, M.; Heise, B.; Ishaya, S.; Laschewsky, A. *J. Am. Chem. Soc.* **2002**, *124*, 3787.
(76) Engin, K.; Leeper, D. B.; Cater, J. R.; Thistlethwaite, A. J.; Tupchong, L.; McFarlane, J. D. *Int. J. Hyperthermia* **1995**, *11*, 211.
(77) Chen, G. P.; Ito, Y.; Imanishi, Y. *Macromolecules* **1997**, *30*, 7001.
(78) Tao, L.; Mantovani, G.; Lecolley, F.; Haddleton, D. M. *J. Am. Chem. Soc.* **2004**, *126*, 13220.
(79) Haddleton, D. M.; Waterson, C. *Macromolecules* **1999**, *32*, 8732.
(80) Bories-Azeau, X.; Armes, S. P. *Macromolecules* **2002**, *35*, 10241.
(81) Smith, M. B. *Organic Synthesis*, 2nd ed.; McGraw-Hill: New York, 2002.
(82) Akiyama, Y.; Nagasaki, Y.; Kataoka, K. *Bioconjugate Chem.* **2004**, *15*, 424.
(83) Lutz, J. F.; Hoth, A. *Macromolecules* **2006**, *39*, 893.
(84) Wang, X. S.; Lascelles, S. F.; Jackson, R. A.; Armes, S. P. *Chem. Commun.* **1999**, 1817.
(85) Butun, V.; Billingham, N. C.; Armes, S. P. *Chem. Commun.* **1997**, 671.
(86) Lee, A. S.; Gast, A. P.; Butun, V.; Armes, S. P. *Macromolecules* **1999**, *32*, 4302.
(87) Butun, V.; Armes, S. P.; Billingham, N. C. *Polymer* **2001**, *42*, 5993.
(88) Butun, V.; Armes, S. P.; Billingham, N. C. *Macromolecules* **2001**, *34*, 1148.
(89) Layer, R. W. *Chem. Rev.* **1963**, *63*, 489.
(90) Sprung, M. A. *Chem. Rev.* **1940**, *26*, 297.

MA071494O